Journal of Materials Chemistry B

Accepted Manuscript

ROYAL SOCIETY OF CHEMISTRY

www.rsc.org/materialsB

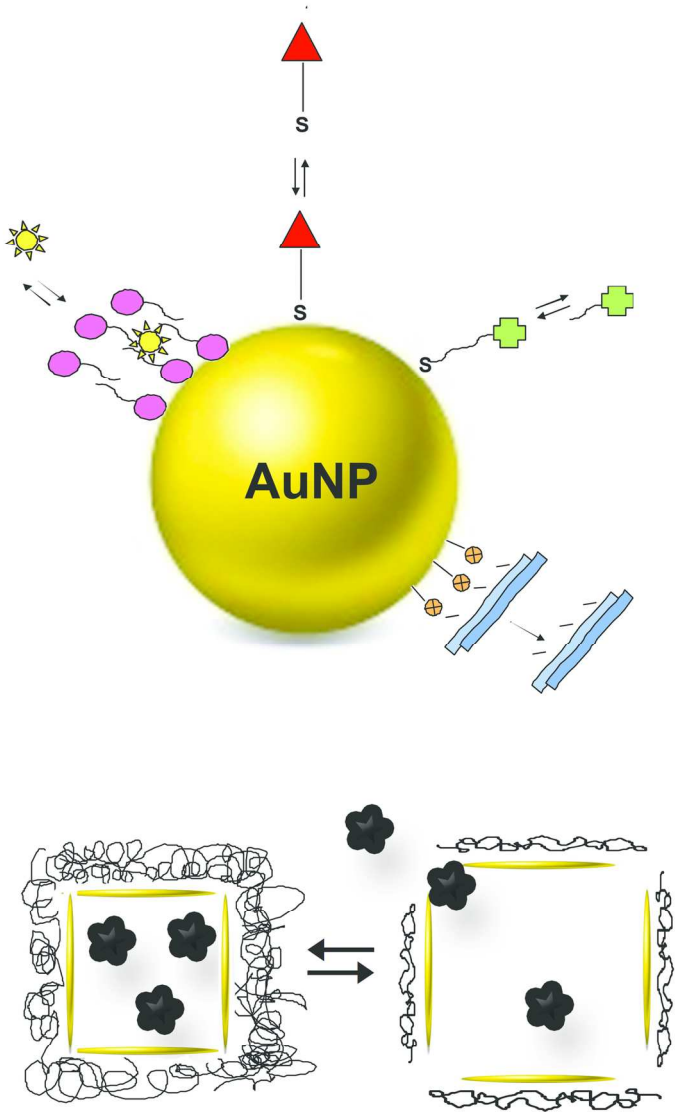

59x90mm (600 x 600 DPI)

Gold nanoparticles and their conjugates as drug delivery vehicles for selective targeting of cancer cells.

Gold nanoparticles and gold nanoparticle-conjugates for delivery of therapeutic molecules. Progress and challenges.

I. Fratoddi,*[a] I. Venditti,[a] C. Cametti,[b] and M. V. Russo[a]

Received Xth XXXXXXXXXX 20XX, Accepted Xth XXXXXXXXX 20XX
First published on the web Xth XXXXXXXXXX 200X
DOI: 10.1039/b000000x

This article reviews the most recent literature data on the applications of gold nanoparticles and their various conjugates which make them suitable structures towards biomedical and clinical purposes, with emphasis in their use as drug delivery vehicles for selective targeting of cancer cells. With the rapid surge in the development of nanomaterials, new methodologies and treatment strategies have been explored and these topics should be taken into consideration when a current scenario is required in the design of new experimental approaches or in a comprehensive data interpretation. We present here a summary of the main properties of gold nanoparticles and their conjugates and the state-of-the-art of non-conventional treatment in targeted drug delivery based on gold nanoparticles as carriers, with the aim to give the reader an overview of the most significative advances in this field.

1 Introduction

Mainly due to their high surface-to-volume ratio, joined to the relatively easiness of their functionalization with targeting ligands, their farmaco-kinetics and tumor tissue accumulation, gold nanoparticles [AuNPs] have been widely used in recent years in biotechnological and biomedical applications [1–3] and, more recently, they have found an expanding field as exploratory drug delivery vehicles [4–6]. AuNPs have about one hundred to ten thousand times smaller size than human cells and consequently they can offer unprecedented interactions with biomolecules, both on the surface and inside biological cells. Applications of AuNPs in biomedicine as medical diagnostics and therapeutics are just beginning to be fully appreciated and their potentiality has not yet fulfilled the great expectation gold nanoparticles provoked, becoming a focus on innovative biomedical research [7].

After a proper functionalization, these particles can be engineered to accumulate preferentially at tumor sites, becoming a new agent in cancer treatment, and providing, moreover, a powerful tool for drug delivery systems or for sensing devices [8–13]. This has resulted in a broad array of studies in which gold nanoparticles have assumed a relevant importance in innovative ways to control the transport and the subsequent release of drugs to specific tissues. These mechanisms are furthermore facilitated by the fact that the release can proceed *via* internal stimuli, such as pH, or *via* external stimuli, such as light or heat [14,15].

[a] *Dipartimento di Chimica, University of Rome "La Sapienza", Rome, Italy. Tel: 39 06 49913 347; E-mail: ilaria.fratoddi@uniroma1.it*
[b] *Dipartimento di Fisica, University of Rome "La Sapienza", and CNR-INFM-SOFT, Rome, Italy.*

The range of uses of AuNPs in medical and biological fields is extremely broad and extensive information on the most important aspects in their synthesis, electrochemistry and optical properties have been so far the subject of various reviews [1,16–20].

This area is however too large for a comprehensive treatment in the space of this review and we have accordingly selected two areas of highlighting interest, *i.e.*, the formation of nanoparticle conjugates and their use as drug carriers, that is one of the most promising aspects in medicine, presenting new challenges and opportunities [3,21–23].

Since both these fields have in the past been covered by excellent reviews, here we narrow the focus to consider only the most recent studies in which gold nanoparticles have been used to bind specific targeting drugs or have been used as new agents for drug or gene delivery.

Here, the term gold nanoparticle(s) [AuNPs] will refer to a collection of differently shaped particles encompassing, beyond spheres, nanorods, nanoshells, nanocages and gold-based nanoparticles, termed SERS nanoparticles, which present surface-enhanced Raman scattering properties. Each of these differently shaped nanostructures exhibits different potential applications in biomedicine, based on their different scattering properties, spectral sensitivity and near-infrared absorption. A comprehensive panel collecting the various types of plasmon-resonant nanoparticles, including gold nanoparticles, is shown in Fig. 1.

In this review, first we will discuss some features of the wide variety of shape and size of gold nanoparticles that render them extremely attractive vectors in cancer diagnosis and therapy and a mean to destroy cancer cells, proving to be of immense potential in diverse arrays of biomedical applications.

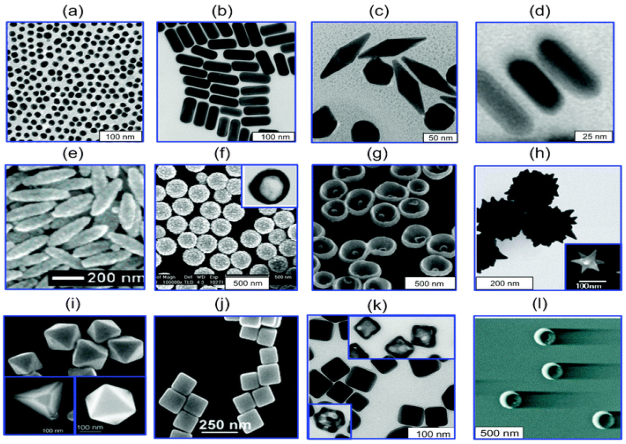

Fig. 1 Various types of plasmon-resonant nanoparticles. (a): nanospheres; (b): nanorods; (c): bipyramids; (d): nanorods covered by silver nanoshells; (e): gold-coated Fe_2O_3 nanorods; (f): SiO_2/Au nanoshells; (g): nanobowls with bottom cores; (h): spiky Fe_2O_3 nanorods; (i): tetrahedra, octahedra and cubooctahedra; (j): gold nanocubes; (k): gold-silver nanocages; (l): gold nanocrescents. Reproduced from Reference [3], with permission from The Royal Society of Chemistry.

We give an overview of the different conjugates that, owing to the unusual optical and electronic properties and potential biomedical applications, have recently received considerable attention. In the following sections, we will illustrate how these nanostructures can be exploited to be promising agents in drug delivery.

2 Gold nanoparticle-based conjugates

With the continuous development of the synthesis technique, gold nanoparticles can be produced with well-controlled size (and size distribution, too), shape and physical properties [24–31]. The current state-of-the-art of gold nanoparticles in biomedical applications is summarized in recent excellent reviews [1,32–34]. The most used nanoparticles include nanospheres (1.5 nm to over 100 nm in diameter or more), nanorods (synthesized using a template method, with diameter and length governed by electrochemical deposition), nanoshells (with surface plasmon resonance peaks ranging from visible to NIR region, due to collective oscillations of their conducting electrons in the presence of an incident light), nanocages (with controlled pores and wall thickness) and SERS nanoparticles (based on Surface-Enhanced Raman Scattering technique).

Among the peculiar characteristics of these particles, it deserves to be mentioned here their ability in the conversion of light to thermal energy [35,36] with the advantage that the wavelength at which the plasmonic heating is maximum can be tuned to the tissue window [37,38]. In Fig. 2, we report the optical extinction of differently shaped gold nanoparticles, showing the shift towards higher wavelength as the shape factor increases, from spheres to nanorods.

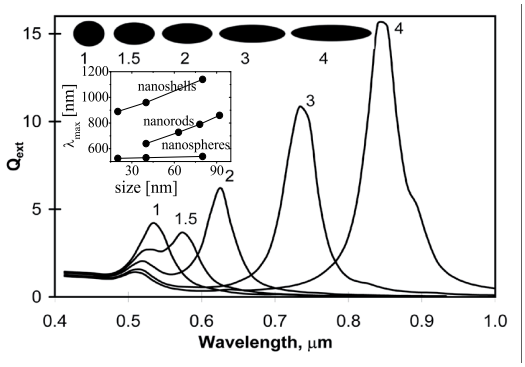

Fig. 2 Calculated optical extinctions of typically-sized gold nanorods of varying aspect ratios in water, but equal volume with an effective radius of 20 nm. The inset shows the variation of surface plasmon extinction maximum λ_{max} as a function of particle size for nanospheres (diameter D), nanoshells (external radius R_2 and shell thickness $R_2 - R_1$=0.143xR_2) and nanorods (long axis length R_2, small axis length R_1=20 nm). Reproduced with permission from Reference [39]. Copyright 2006 Wiley-VCH Verlag GmbH Co.

Gold nanoparticle surface represents one of the most easily functionalized platform, where conjugation is possible with a variety of organic self-assembled monolayers (thiolates, amines, carboxylates, cyanides, etc), with an adsorbate coverage that can be as high as 10^{15} molecules/cm^2 [40]. Once functionalized with appropriate ligands (for example, poly(ethylene glycol), which is one of the most common surface ligands), gold nanoparticles are stable enough in physiological environment with high ionic and serum concentrations, exhibit high circulatory half-lives, besides a decreased immunogenic response and a reduced recognition and removal by the mononuclear phagocyte system. All these characteristics are prerequisites for specific tailoring in nanomedical applications and allow gold nanoparticles to act as highly multifunctional anti-cancer agents.

In the following, we briefly list the main methods to realize nanoconjugates with properties and characteristics that are being valuated for drug delivery and cancer treatment. In doing this, we will follow the scheme suggested by El-Sayed and coworkers [41] in their excellent and comprehensive review with the fascinating title "*The golden age: gold nanoparticles for biomedicine*".

A summing up panel showing the different approaches to loading and release of therapeutics into and from gold nanoparticles is illustrated in Fig. 3. The diverse functional

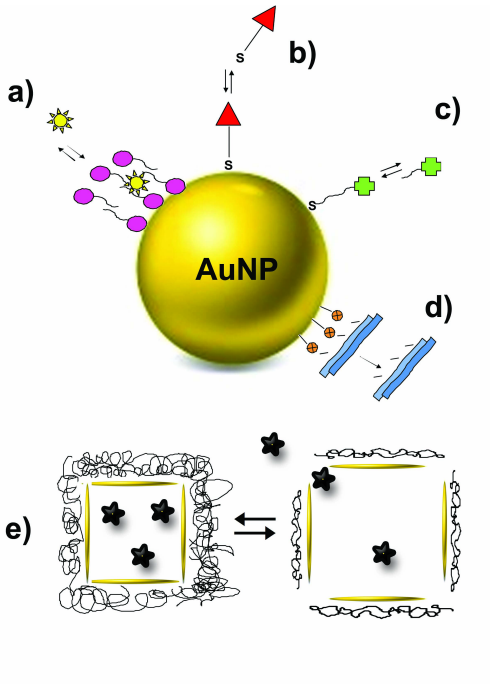

Fig. 3 Cartoon showing different approaches to loading and unloading therapeutic molecules in gold nanoparticles. (a): partitioning and diffusion of hydrophobic molecules in a surfactant bilayer; (b): surface complexation, by anchoring drugs through Au-S (or Au-N) bonds; (c): drugs complexed to functional groups of capping agents; (d): loading by electrostatic conjugation and electrostatic assembly; (e): gold nanocages (hollow cubes with porous walls). Heat induced by exposure to near-infrared laser produces a collapse of the themosensitive polymers and the release of the drugs incorporated within the particle.

possibilities, due to the functional versatility of gold nanoparticle surface, provides an excellent platform for different approaches in the design of the drug delivery systems. The most relevant of them will be briefly commented in the following subsections.

2.1 Loading by partitioning.

Gold nanoparticles are generally coated by a monolayer or a bilayer of a capping agent that prevents aggregation. This coating, which is able to partition hydrophobic molecules from the surrounding aqueous medium, is advantageous to load drugs to be released at the desired target.

For example, Alkilany et al.[42] prepared gold nanorods covered by a surfactant bilayer of cetyltrimethylammonium bromide [CTAB], about 3 nm thick. The presence of the hydrophobic core of the CTAB bilayer on the nanorod surface provides an excellent site for the uptake of water-insoluble molecules from the aqueous bulk. The system is able to partition into the CTAB bilayer hydrophobic molecules, such as 1-naphthol, with a ratio 1.6:1. In this case, the maximum number of bound 1-naphthol molecules is $14.6 \pm 2.2 \times 10^3$ molecules per gold nanorod, with an equilibrium binding constant of $1.97 \pm 0.79 \times 10^4$ M^{-1}, at room temperature.

The uptake of organic molecules from the bulk aqueous phase by gold nanoparticles has useful implications for biomedical applications of these new materials. A typical example has been described by Kim et al.[43] who produced gold nanoparticles capped with a polymer layer with a hydrophobic interior region and a hydrophilic exterior region. The concurrent presence of both hydrophobic and hydrophilic layers facilitates the loading of hydrophobic drugs on one side and the stabilization of nanoparticles in aqueous media on the other side. In this case, the drug release occurs by means of a repartitioning of the drug from the hydrophobic region of the polymer layer to the hydrophobic domain of the cell membrane, without the need for the particle to enter the cell.

AuNPs functionalized with a polymer layer that can be either a binary mixture of homopolymers or diblock copolymers have been recently reviewed by Chen and Klok[44], who termed "multifaceted" these two-component polymer-modified systems. The presence of this two-component polymer coating offers a further possibility in modulating nanoparticle properties suitable for various bio-relevant applications[45]. A typical example has been reported by Boyer et al.[46] who were able to modulate the surface charge of AuNPs modifying their surface with a mixture of a charged polymer and a neutral, thermosensitive polymer, resulting in a ζ-potential that can be tuned from 0 to +30 or to -20 mV in the temperature range from 5 to 35 °C. The difference in the ζ-potential, and hence in the surface charge, can greatly promote and, partially, favor interaction with cell membrane. The greater the ζ-potential the more likely the particle suspension is to be stable or, conversely, interactions with oppositely charged objects become relevant.

A further example of the large versatility of these systems has been reported by Boyer et al.[47,48] who described the thermal behavior of AuNPs modified with a mixed brush of two thermosensitive polymers. They employed poly(diethylene glycol) acrylate (with a lower critical solution temperature [LCST] of 15 °C) and a copolymer composed by poly(diethylene glycol) acrylate and oligo(ethylene glycol) acrylate (with a LCST of 35 °C) [poly(DEG-A) and poly(DEG-A-co-OEG-A)]. The system reveals two completely reversible hydrophilic to hydrophobic transitions, localized around 8-10 °C and 25-20 °C, respectively. At higher temperatures, a destabilization of the mixed structures yields to aggregation. This thermal behavior, that shows a dual temperature responsiveness, can be appropriately exploited in thermosensitive gold nanoparticles, leading to significantly different interactions and accumulation in different biological

organs[47,48].

These examples serve to give a first taste of the many exciting possibilities that gold biospecific-conjugate nanoparticles exhibit in cancer treatment. In this context, a layer-by-layer technique has been used by Takahashi et al.[49], who modified phosphatidylcholine-gold nanorods [PC-NRs] with bovine serum albumin [BSA] and polyethylenimine [PEI]. The stability of gold nanoparticles in saline solution was greatly increased when BSA-PC-NRs were wrapped inside PEI by means of a layer-to-layer technique, resulting in an increased cellular binding and uptake under physiological conditions.

2.2 Loading by surface complexation.

Drugs complexed with thiols or free amines can be loaded to gold nanoparticles taking advantage of the formation of Au-S or Au-N bonds that these complexes form at the particle surfaces. For example, this methodology has been applied to attach different drugs[50–52] or DNA[53,54].

Au-S or Au-N bonds have a different strength and this fact can be conveniently used to modulate in a rather controlled fashion the drug release profile. If a retarded profile is preferred for therapeutical advantage, Au-S bond is better. In some cases, the presence of Au-S bonds needs an external stimulus to allow the complexed drug could be released. Different delivery profiles when drugs are attached to the gold surface through Au-S or Au-N bonds have been described by Cheng et al.[50], who claimed attention on the fact that, whereas labile amino adsorption to gold nanoparticles allows efficient drug release into the cancer cells (for example, in the framework of the photodynamic therapy [PDT]), a covalent thiol bond leads to the delivery of the drug into cell vesicles, and no PDT effect is observed. This finding suggests caution in choosing the appropriate interaction between drug molecules and the nanoparticle surface.

Moreover, surface complexation by means of thiols or free amines offers the further advantage that both the loading and the release processes can be properly monitored by simple fluorescence microscopy (if drugs are fluorescent) or by Surface-Enhanced Raman Spectroscopy [SERS]. In fact, gold nanoparticles have the unique properties of enhancing the Raman signal of adsorbed dye molecules on their surface, allowing the detection of picomolar amount of the target analyte, up to a single target molecule[55]. Moreover, SERS provides detailed spectroscopic information that can be adapted to an *in vivo* imaging system[56].

As a further approach, Kim et al.[43] chose three different hydrophobic guest compounds, i.e., 4,4-difluoro-4-bora-3a,4a-diaza-s-indacene [Bodipy] (as a fluorescent probe), and two highly hydrophobic therapeutics, tamoxifen [TAF] and β-lapachone [LAP], as drugs, demonstrating that hydrophobic dyes/drugs can be stably entrapped in a hydrophobic pocket of AuNPs and released into the cell by membrane-mediated diffusion, without uptake of the carrier nanoparticle.

It is also worth noting that particle solubility in water and in a broad range of polar organic solvents can be obtained employing gold nanoparticles passivated with thiol-terminated poly(ethylene glycol) [PEG][57]. Oh et al.[57] investigated the effect of the polymer molecular weight and the thiol-to-gold molar ratio on the size of gold nanoparticles capped by polymeric thiols. Using PEG spacers, the gold nanoparticles can be conjugated with a variety of biological relevant ligands (fluorescent dyes, antibodies etc.) in order to target, probe and induce a stimulus at the target site[58].

2.3 Loading by attachment to capping agents.

In this case, the terminal functional groups of capping agents act as drug attachment points. After the particle surface is passivated with these functional groups, the drug interacts with the resulting outermost layer on the top of the particle.

Gold nanoparticles have been conjugated to a variety of antitumor substances. For example, Oxaliplatin, a platinum-based anticancer drug, has been proved to be an important chemiotherapic drug, even if suffering by severe side-effects. Brown et al.[59] employed nanoparticles funtionalized with a thiolated poly(ethylene glycol) [PEG] monolayer capped with a carboxylate group. Addition of this drug to the PEG surface resulted in a complex containing about 300 drug molecules per nanoparticle, which demonstrated an enhanced ability to penetrate the nucleus of lung cancer cells[60], greatly reducing adverse side-effects.

In another example, platinum anticancer agents were complexed to the carboxylic acid moieties from the capping agents in order to prepare platinum-tethered gold nanoparticles able to kill lung and colon cancer cells[61].

Nitric oxide [NO]-releasing gold nanoparticles have been proven to have potential application in vasodilation[62,63]. Schoenfisch and co-workers[62,63] synthesized $3 \div 5$ nm water-soluble NO-releasing gold nanoparticles by attaching NO donor molecules, such as N-diazeniumdiolate, to the terminal amines on gold nanoparticles. These conjugates represent an important step toward developing NO-release scaffolds for biological applications. As demonstrated by these authors[62,63], polyamine-protected gold clusters facilitate the storage and release of NO at levels equivalent to larger water-insoluble scaffolds (e.g., silica and polyethyleneimine microspheres, with size of the order of 200 μm).

Finally, it deserves to be mentioned here the work by the Rotello group[64], where an anticancer drug (5-fluorouracil, [5FU]) was attached to gold nanoparticles with terminal carboxylic acid groups from the capping agent, through a photosensitive *o*-nitrobenzyl linkage.

This approach, however, is not free from some inconveniences. In fact, as pointed out by Dreaden et al.[41], the coupling of drugs (or therapeutics, as well) to the capping agents on the nanoparticle surface can result in particle aggregation, thus reducing the overall solubility of these complexes in water with the consequence of a decreased release capability.

2.4 Loading into the interior of nanoparticles.

Besides gold (bulk) nanoparticles, hollow gold nanostructures, with the presence of an internal reservoir, are suitable for drug delivery applications, because of their capability to load drugs. Among these structures, it deserves to be mentioned here gold nanocages [AuNCs][65] and gold nanoshells [AuNSs][66,67]. As far as the formers are concerned, Yavuz et al.[65] developed an interesting system based on gold-nanocages covered by smart polymers anchored to the gold surface by means of gold-thiolate linkage. These authors used poly(N-isopropyl-acrylamide) and its derivatives, whose conformation may change in response to small variation of temperature. As a consequence, the preloaded effector can be released in a very effective and controllable way using a near-infrared laser whose light is absorbed and converted into heat by photothermal effect. The method presents a high spatial and temporal resolution and, moreover, nanocages can be functionalized with targeting ligands such as antibodies[65].

As a further example, we mention the strategy for loading either hydrophobic or hydrophilic drugs developed by Moon et al.[66]. This method is based on the use of a phase-change material [PCM] which loads and releases the drug in response to a thermal increase due to heating by thermal, photothermal or ultrasonic means. Since PCM reversibly changes its physical state between solid and liquid over a narrow temperature range, it can confine drug molecules inside the gold nanocages at a temperature below its melting point. When the local temperature is raised beyond the melting point of the PCM, it will begin to melt and the drug will be released from the melted PCM through simple diffusion. This system has the further advantage of regulating the release of drug and its profile by manipulating the temperature. As long as the drug is miscible with the PCM phase, it can be conveniently loaded into the hollow interiors of AuNCs as the PCM diffuses into the nanocages. This requirement can be readily met by choosing PCMs with a surfactant-like behavior such as those containing both long hydrophobic tails and hydrophilic heads. These authors[66] chose 1-tetradecanol, a fatty alcohol characterized by its immiscibility with water, but mixible with hydrophilic and hydrophobic substances, good biocompatibility and melting point slightly higher than the normal human body temperature. Fig. 4 shows the release profile of Rhodamine 6G induced by a thermal heating. As can be seen, as the temperature increases above the human body temperature, a pronounced drug release occurs. The system is highly sensitive to temperature, being the release increased from 5% to 28% for a temperature increase from 37 to 40 °C.

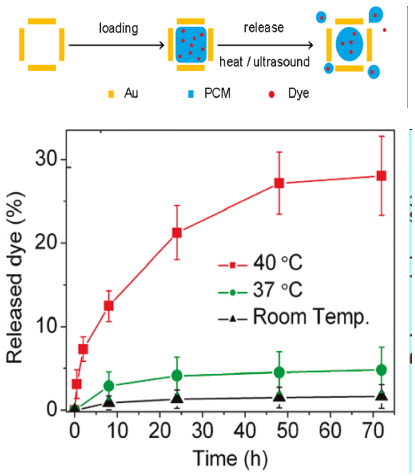

Fig. 4 Upper panel: Schematic illustration of how to load the hollow interior of an AuNC with a dye-doped PCM and then to have it released from AuNC by direct heating. Bottom panel: Release profile of Rhodamine 6G under direct heating to various temperatures as a function of time. Reproduced with permission from Reference[66]. Copyright 2011 American Chemical Society.

2.5 Loading by charge interactions.

Because of the presence of capping agents on their surface, gold nanoparticles bear a surface charge making this system suitable for electrostatic conjugation with oppositely charged drugs.

The classic example of this loading mechanism is the attachment of DNA chain to the gold nanoparticle surface, by virtues of its polyelectrolyte character[67]. The comparable size of DNA and small functionalized nanoparticles facilitates their interaction[68,69]. Ghosh et al.[70] have demonstrated that quaternary ammonium-functionalized gold colloids effectively recognize DNA strands. Nanoparticles bearing primary ammonium groups (pKa $\simeq$ 10) on the surface are also expected to bind with anionic DNA, via ion-pairing at physiological pH (pH = 7.4)[71].

Gold nanorods rapidly aggregate in biologically relevant media. Huang et al.[72] demonstrated that the deposition of polyelectrolyte multilayers on gold nanorods enhanced the stability of these nanoparticles at least up to 4 weeks. Moreover, dispersions of polyelectrolyte (PE)-gold nanorod assem-

blies (PE-AuNRs) show higher transfection efficiency and lower toxicity compared to those based on polyethyleneimine. These authors[72] concluded that engineering of biocompatible polyelectrolytes leads to functional gold nanorod-based assemblies that combine high stability, low citotoxicity, photothermal ablation and gene delivery.

This broad range of methods allowing the loading and the release of therapeutics we have listed here is the basis of the extraordinary interest gold nanoparticles have rouse in biomedical nano-technology.

3 AuNPs as carriers for delivery of therapeutic molecules.

The delivery of anticancer drugs and other therapeutic molecules is one of the most promising goals for gold nanoparticles that are expected to give dramatic results in therapy to deliver a variety of anticancer substances, conjugated by simple physical adsorption or by using thiol linkers. This rapidly expanding field is essentially due to the capability of gold nanoparticles to bind a wide range of organic molecules, to their low-level of toxicity and to their strong and tunable optical adsorption. Further, as mentioned above, with the size of about one hundred to ten thousand times smaller the ones of than human cells, gold nanoparticles can offer a wide spread of interactions with biomolecules both at the surface and inside the cells, making this methodology central in cancer treatment[73].

One of the main advantages of gold nanoparticles is that they present a higher intracellular uptake than microsized particles. Through both passive and active targeting, the drug concentration can be increased at the tumor site, while limiting the exposure of healthy tissues, with a consequent reduced toxicity. This has special implications for gene delivery, as DNA can be easily encapsulated and transfected with a high efficiency. In particular, AuNPs have the correct size to pass by passive diffusion in tumor vasculature, increasing the residence time of any toxic agent eventually carried by the nanoparticles themselves within the tumor mass.

The cellular uptake and cell membrane penetration is governed by three interconnected parameters, i.e., surface charge density, particle size and shape, and finally particle surface functionality. The influence of these parameters, that must be appropriately considered during the nano-formulation in order to minimize toxicity and to increase therapeutic effects, has been investigated by several authors. In particular, the role of the surface charge has been studied by Cho et al.[74], Chompoosor et al.[75] and Ghosh et al.[70], while the size dependence and the surface functionalization have been investigated by Jiang[76], Verna et al.[77] and by Nativo et al.[78].

As far as the influence of the particle size is concerned, the complexity of the phenomenology involved is clearly evidenced in the study by Chen et al.[79], who reported the *in vivo* effect of naked gold nanoparticles of size from 2 to 100 nm injected in BALB/C mice (at the dose of 8 mg/(Kg week)). They found that, while AuNPs with size in between 10 and 40 nm caused acute toxicity, both smaller particles and larger particles did not show any apparent toxicity, without death during the observation period.

Differently functionalized nanoparticles behave differently. For example, the pharmacokinetics of AuNPs functionalized by mPEG was investigated by Perrault et al.[80] in tumor bearing CD1 mice and these authors observed that the half-life of smaller particles was eight-fold higher compared with the ones of larger particles. These results were confirmed by Zhang et al.[81] supporting that, in nude mice, PEG-AuNPs 20 nm in size had a longer half-life than nanoparticles 40 and 80 nm in size.

The field is even more intricate, as far as the surface characteristics are concerned, since the electrical charge of AuNPs greatly influences their behavior. Experiments carried out by Balogh et al.[82] in mice injected with positive, negative and neutral surface charged AuNPs, with size varying between 5 and 22 nm, have shown that the highest particle retention in blood was obtained with positive 5 nm in size particles. Moreover, positive nanoparticles accumulate preferably in kidney, whereas positive and negative particles preferred a statistically significant accumulation in the liver.

The particle bio-distribution too is greatly influenced by size and surface charge. An injection of radio-labeled gold nanoparticles of various sizes in the range 1-200 nm in rats was implemented by Hirn et al.[83]. They administered ^{198}Au-radio-labelled monodisperse, negatively charged AuNPs of five different sizes (1.4, 5, 18, 80, and 200 nm) and 2.8 nm AuNPs with opposite surface charges, by intravenous injection into rats. After 24 h, the biodistribution of the AuNPs was quantitatively measured by gamma-spectrometry technique. Fig. 5 shows some typical results, for some selected organs. As can be seen, particle size influences differently selected organs and the different accumulation has a varied pattern. For AuNPs between 1.4 and 5 nm, the accumulation increased sharply with decreasing size, i.e., a linear increase with the volumetric specific surface area. The differently charged 2.8 nm in size particles led to significantly different accumulation in several organs.

Another example concerns with citrate capped gold nanoparticles of sizes in the range 15 - 200 nm. These particles were used by Sonavane et al.[84] for the measurement of the permeation coefficient in *in vivo* permeation experiments. Particle distribution demonstrated that, in this case, larger particles remained close to the surface of the skin, whereas smallest particles were found in the deep region of the skin.

These results, as a whole, confirm that, due to the complexity and the overlapping of the different effects, a strategic

methodology has been not yet developed and further experimental work is necessary before a successful translation of nanoparticles to the clinics could occur.

3.1 Gold nanoparticles for gene delivery.

Gold nanoparticles have long been regarded as alternative non-viral vectors and attracted a great interest as non-viral gene delivery because of their unique properties.

In particular, it has been shown that nanoparticles functionalized with cationic quaternary ammonium groups are able to bind plasmid DNA through electrostatic interactions (by non-covalent interaction), to protect DNA from enzymatic digestion and to release the bound DNA by glutathione treatment in cuvette [69,85,86].

It has been reported that nucleic acid strands could be easily modified with thiols (SH) for grafting onto nanoparticles, by covalent linking [87]. In this context, Niidome et al. [88] prepared cationic gold nanoparticles complexed with plasmid DNA containing a luciferase gene and the complex has been proved to be efficient in delivering a gene into the target HeLa cells. The same gold nanoparticles, whose stability was increased by addition of polyethylene glycol orthopyrydil disulfide [PEG-OPSS] during the DNA conjugation, were employed in combination with laser irradiation (power density of 80 mJ/pulse) without any DNA fragmentation, during the nucleic acid release [21,89].

As noted above, gold nanoparticles have a strong and tunable surface plasmon absorption in the NIR range. A demonstration that plasmid DNA can be released from nanorod particle surface induced by NIR irradiation has been given by Wijaya et al. [90].

By conjugating two different DNA oligonucleotides to short and long gold nanorods, presenting longitudinal plasmon resonances with light at 800 and 1100 nm, respectively, these authors [90] succeeded in a selective melting when irradiated with light at a wavelength corresponding to the appropriate resonance. After laser irradiation at the wavelength of 800 nm, about 70 % of the DNA attached to the short rods was released while only about 10 % of the DNA conjugated to long rods was released. This finding further confirms that the selective release from gold nanorods could be a new and powerful technique to improve gene delivery.

Another interesting approach to improve gene delivery using gold nanoparticles has been reported by Kawano et al. [91], who used gold nanoparticles modified with mPEG-SH_{5000} and conjugated with plasmide DNA. After injection of the composite in an anesthetized mouse, excitations with electrical pulses to the left lobe of its liver produced the gene expression in its major organs. On the contrary, injection of naked DNA resulted in more than ten-fold lower level of detection.

Likewise, in another study, plasmid DNA encoding murine interleukin-2 (pVAXmIL-2) was mixed with positively charged gold nanoparticles, increasing the transgene expression significantly and, moreover, with a reduced toxicity [92].

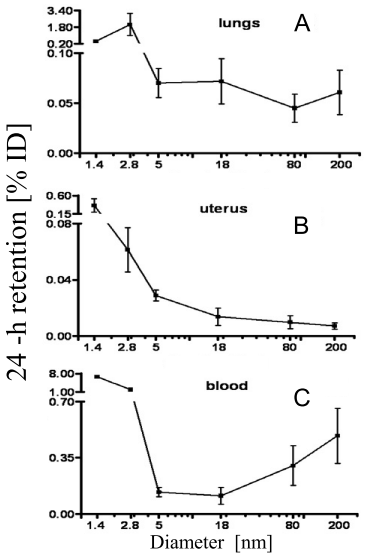

Fig. 5 Twenty-four hours retention of intravenously injected, negatively charged, spherical AuNPs (1.4 nm, 5 nm, 18 nm, 80 nm, 200 mm coated with mono-sulfonated triphenylphosphine [TPPMS]; 2.8 nm carboxyl-coated). In each panel, the respective organ is indicated. Data are mean ± SD, n = 4 rats. Note log scale of x-axis. Reproduced from Reference [83]. Copyright 2011, with permission from Elsevier.

Higher transfection efficiency for gene delivery was achieved when DNA was conjugated on AuNPs complexed with polyethyleneimine [PEI] and with chitosan [93]. In particular, AuNPs functionalized with PEI have been used as a gene delivery vector with a reduced cytotoxicity in rabbit cornea, where tissues collected after different time intervals, up to 7 days, showed a relevant amount of gold particles in keratocytes and in extra cellular matrix of rabbit cornea. Nanoparticles functionalized at a different extent with PEI with varying alkyl chain lengths enhanced (up to 26-fold) the *in vivo* gene expression efficiency in mouse lungs [94].

Recently, graphene oxide [GO] has attracted great attention in biomedical applications as gene delivery [95]. A strategy for the fabrication of GO-encapsulating gold nanoparticles by electrostatic self-assembling between negatively charged GO nanosheets and positively charged gold nanoparticles has been developed by Xu et al. [96]. The grafting of polyethylenimmine [PEI] onto the GO surface allows the complex to be suitable for gene delivery. These PEI-functionalized GO-encapsulating AuNPs presented very low toxicity and high transfection efficiency in He-La cells.

3.2 Gold nanoparticles for cancer therapy and synergic anticancer drug delivery.

Cancer treatment based on gold nanoparticles has the primary advantage of minimizing the damage of neighboring non-cancerous tissues, the treatment being applied directly to the tumor, leaving surrounding tissues practically unaffected. These treatments mainly include photodynamic therapy[97] and regional hyperthermia[98].

While the former is achieved by focusing a light source absorbed by tissues (wavelength 630-900 nm, near infrared region [NIR]) on a particular region of the body, the latter is characterized by the damage of the cells from exposure to elevated temperatures, causing loss of membrane integrity, DNA damage and finally cellular death. In both these fields, gold nanoparticles hold great promise, overcoming the difficulties of achieving a localized heating of the tissue.

In addition to facile surface modification and their large surface-to-volume ratio, AuNPs also possess a number of other properties that can be used in drug delivery applications.

Plasmonic photothermal therapy [PPTT] is a minimally-invasive oncological treatment strategy in which photon energy is selectively administered and converted into heat, sufficient to induce cellular hyperthermia. This emerging anticancer treatment is based on the use of gold nanoparticles that, once accumulated in the target, are able to absorb light strongly within the tissue-transparent near infrared region[99]. The treatment with nanoparticles and their subsequent irradiation with near-infrared laser produces heat sufficient to induce tumor ablation (i.e., irreversible damage to the cells, caused by disruption of cell membrane and protein denaturation).

When irradiated with laser pulses of appropriate wavelength, electrical currents are produced in the gold nanoparticles, creating a rapid heating which quickly dissipates from the particles into the surrounding tissues, producing thermal ablation. Temperatures as high as 70-80 °C can be easily achieved and gold nanoparticles can kill bacteria and cancer cells[100,101].

The pioneering work of Hirsch et al.[102] demonstrated that the exposure of human breast carcinoma cells, treated with gold nanoparticles (nanoshells), to low dose of NIR light, resulted in an increase of temperature (up to an increment of 30 °C) capable of inducing irreversible tissue damage. Since then, the effectiveness of this technique in the treatment of different types of cancer has been confirmed by Stern et al.[103,104] and by O'Neil et al[37].

The following few examples among many others reported in the literature are illustrative of aims and perspectives. As pointed out by Cai et al.[73], plasmonic photothermal therapy [PPTT] involves only passive tumor therapy, with a non-specific accumulation of nanoparticles in the cancer tissue (enhanced permeability and retention effect, [EPR] effect), due to the characteristics of the tumor vasculature[105].

Particularly relevant, the study carried out by Raji et al.[106], who employed citrate capped AuNPs, 15 nm in size, to treat human epithelial cancer cells (A413 cells) exposed to low laser light at different time intervals. After laser irradiation, cell morphology changes were examined using phase contrast microscopy along with the relevant biochemical parameters, like lactate dehydrogenase activity, reactive oxygen species generation and caspase-3 activity. These authors[106] concluded that these nanoparticles could selectively induce cell death via reactive oxygen species [ROS] mediated apoptosis.

Beside photothermal therapy, gold nanoparticles have been also investigated in other therapeutic studies[107]. In a different context, Agostinelli et al.[108] developed a new immunotherapeutic pathway against human osteosarcomas and melanomas that takes advantage of the high polyamine content in cancer cells. Amine oxidases purified from bovine serum [BSAO] have been used for the generation of polyamines and new strategies based on Fe_2O_3 nano-carriers are under study to find how the enzymes could be delivered *in vivo* in clinical applications[109].

The use of light as an external stimulus to release a drug from gold nanoparticles is based on the fact that these systems undergo a strong plasmon resonance with light. Moreover, the peak of this absorption can be easily shifted from the middle of visible wavelength (500 nm) to the near-infrared (800-1200 nm) by changing the particle shape from spherical to more complex shapes, for example rods or nanoshells (see, for example, Fig. 2). As far as these latters are concerned, these spherical nanoparticles consist of a dielectric core covered by a thin metallic shell, which is typically gold.

In addition to spectral tunability, nanoshells offer other advantages over conventional organic dyes, including improved optical properties and reduced susceptibility to chemical/thermal denaturation. This strategy was adopted by Loo et al.[110] and by O'Neil et al.[37] who investigated the use of nanoparticle-assisted photo-thermal therapy [PPT]. The former group[110] describes several examples of absorbing nanoshells in NIR thermal therapy of tumors. In particular, absorbing nanoshells at the concentration of 10^9 particles/mL, were injected into solid tumors in female SCID mice. Tumor sites were then exposed to NIR light (λ=820 nm, 4 W/cm^2) and consequently temperature reached values that caused irreversible tumor damage.

The latter group[37] employed polyethylene glycol coated nanoshells (with a diameter of the order of 130 nm) with peak optical absorption in the NIR that were intravenously injected and allowed to circulate for 6 h in the tumor vasculature grown in immune-competent mice. When illuminated with a diode laser (808 nm, 4 W/cm^2, 3 min), all tumors were ablated and treated mice appeared healthy up to 90 days later.

Besides gold nanospheres, gold nanorods [AuNRs] too have

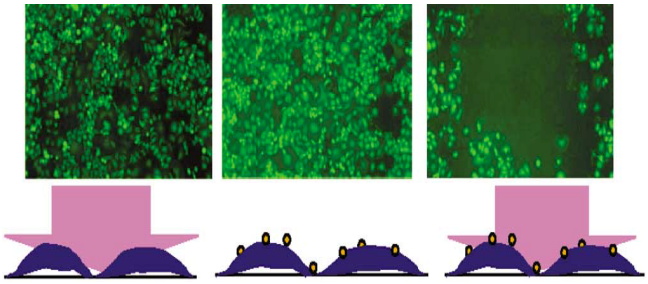

Fig. 6 Calcein AM staining of cells (green fluorescence indicates cellular viability). Left: cells after exposure to laser only (no nanoshells). Middle: cells incubated with nanoshells but not exposed to laser light. Right: cell incubated with nanoshells after laser exposure. The dark circle seen in the image on the right corresponds to the region of cell death caused by exposure to laser light after incubation with nanoshells. Reproduced with permission from Reference [110].

properties which make them attractive candidates for photothermal therapy. Whereas spherical gold nanoparticles do exhibit plasmon resonance in the mid-visible, and therefore outside of the tissue window, and the efficiency of heating is relatively low (compared to nanorods or nanoshells)[111], nanorods overcome these limitations.

Photothermal destruction of carcinoma cells treated with gold nanoshells is shown as an example in Fig. 6. After laser exposure (35 mW/cm^2 for 7 min) cells underwent a photothermal destruction as ascertained from calcein AM staining, indicating that cell are not viable [110].

An interesting light-sensitive drug delivery system has been achieved by Agasti et a.[64] who employed gold particles with a core diameter of about 2 nm. The surface functionality is guaranteed by a self-assembled monolayer of photo-clevable and zwitterionic thiol ligands, which confers stability and provides water solubility and biocompatibility. The anticancer drug (in this case, 5-fluorouracil, [5-FU]) is conjugated to the particle surface through the terminally anchored ortho-nitrobenzyl group. This group possesses a long-term stability in biological environment, but undergoes a photolytic cleavage when exposed to an UV (265 nm) radiation. Taking advantage of this feature, a photo-controlled release of 5-FU molecules is obtained, as monitored by UV-vis spectroscopy measurements. A clear evidence of this process is attained by exposing nanoparticle solution to alternating periods of light and dark, as shown in Fig. 7. In this case, the effectiveness of the bioconjugate as a photocontrolled drug delivery system was evaluated in MCF-7 cell culture.

A light responsive polymer-nanorod camposite was used by Hribar et al.[112] to trigger the release of a chemotherapeutic drug (doxorubicin) induced by near infrared exposure. In par-

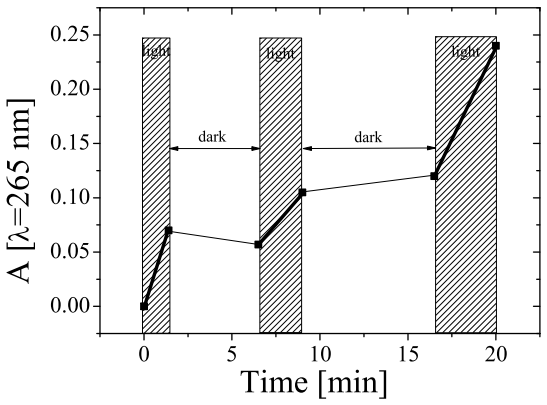

Fig. 7 Change in absorbance due to the formation of 5-FU molecules produced in a glass vial containing a 2.5 μM aqueous solution of 5-FU-conjugated AuNPs exposed to alternating period of light (UV lamp, λ=265 nm) and dark (no light). Adapted with permission from Reference [64]. Copyright 2009 American Chemical Society.

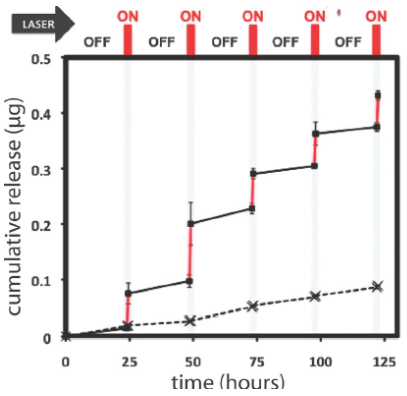

Fig. 8 Experiential results showing drug release as a function of laser irradiation cycles/duration for a microsphere matrix containing gold nanorods. Gold nanoparticles in a composite material are enable to perform light-triggered drug delivery. Gold nanorods distributed in a polymeric microsphere matrix act as localized nanoheaters upon light irradiation. Gold nanorods absorb light and convert it into heat which changes the polymeric matrix from a glassy phase to a rubbery phase, allowing enhanced drug diffusion and release. [Squares]: with laser; [X]: no laser. Laser λ_{max} = 808 nm; Adapted with permission from Reference [112]. Copyright 2012 American Chemical Society.

ticular, at normal body temperature, the polymeric matrix of the composite is in a glass structure and the drug release is limited. On the contrary, at higher temperatures, the polymer is rubbery with a consequent increase of the drug release. Passing from glass to rubber structure is due to the photothermal effect with the conversion of NIR light to heat. A typical example of the process is shown in Fig. 8, where the light-dependent drug release is clearly evidenced. As noted by the authors [112], this approach can be used with different polymeric materials, suggesting the possible development toward clinically applicable therapies.

Dickerson et al. [113] have demonstrated the feasibility of *in vivo* near-infrared plasmonic photothermal therapy [PPTT] using colloidal gold nanorods in an animal model. Subcutaneous squamous cell carcinoma xenografts were grown in nude (nu/nu) mice and the particles were selectively delivered to tumors by both direct and intravenous injection. Thiolated poly (ethylene) glycol (PEG_{5000}) was covalently bound to the gold nanorod surface to increase biocompatibility, to suppress immunogenic responses, and to decrease adsorption to the negatively charged luminal surface of blood vessels. Near-infrared PPTT was performed extracorporally using a continuous wave diode laser. Making use of the enhanced permeability and of the retention (EPR) effect, preferential accumulation of pegylated gold nanorods in tumor tissues was achieved due to the high density, extensive extravasation, and inherently defective architecture of the tumor vasculature, as well as the diminished lymphatic clearance from associated interstitial spaces. Significant decreases in tumor growth were observed for both direct tumor injection (Student test, $P<0.0001$) and intravenous ($P<0.0008$) treatments. Inhibition of average tumor growth for both delivery methods was observed over a 13-day period, with resorption of $>57\%$ of the directly-injected tumors and of 25% of the intravenously-treated tumors.

AuNPs have been conjugated to a variety of antitumor drugs, including paclitaxel [5], cisplatin [114], oxaliplatin [61], doxorubicin [115] and many others. A list of the most common antitumor substances conjugated with AuNPs, together with the method of functionalization, is reported by Dykman and Khlebtov in their recent critical review [116], which witnesses the worldwide efforts and open challenges in the research to defeat cancer.

A strategy which offers a significant potential in the treatment of cancer founded on platinum-based anticancer drugs, such as cisplatin, carboplatin and oxaliplatin, has been recently suggested by Brown et al. [61] who employed gold nanoparticles as carriers, thus reducing the severe dose-limiting side-effect observed with these drugs. The strategy consists in using gold nanoparticles functionalized with a thiolated poly(ethylene glycol) monolayer capped with a carboxylate group. The addition of the drug (oxaliplatin, in this case) to the particle surface yielded a supramolecular complex with about three hundred drug molecules per nanoparticle (platinum-tethered nanoparticle with diameter of 175 ± 25 nm). These platinum-tethered nanoparticles were investigated for cytoxicity, drug uptake and localization in different cancer cell lines, such as lung epithelial and colon cancer cell lines.

Visaria et al. [117,118], with the aim of minimizing the systemic toxicity of tumor necrosis factor-alpha [TNF-α], a cytokine with a pronounced anticancer efficacy, employed PEG coated gold nanoparticles loaded with this drug.

Ionizing radiation is a common treatment for cancer, despite the presence of numerous side-effects and, moreover, the damage of healthy tissues. In this case too, gold nanoparticles offer advantages because of their particular optical properties, surface plasmon resonance and wavelength tunability. A strategy to kill cancer cells without harming the surrounding healthy tissues is based on the employment of gold nanoparticles that, upon X-ray irradiation, induce cellular apoptosis, thorough the generation of radicals [119–121]. For example, Kong et al. [121] developed nanoparticles with modified surface properties (Cysteamine [AET]-capped gold nanoparticles (AET-AuNPs)) and thioglucose capped gold nanoparticles (Glu-AuNPs with an average size of about 10.8 nm), to achieve targeted delivery at the subcellular level. These authors showed that AuNPs significantly increased the cytotoxicity of 200 kV X-rays with at least three benefits, i.e., a higher local concentration of AuNPs in target locations, an increase of the cytotoxicity of radiation, and, finally, a decrease of the local damage to normal tissue surrounding the cancer. The survival rate of MCF-7 breast-cancer cells employed in this experiment is shown in Fig. 9 that demonstrates, in the case of Glu-AuNPs, how these particles enhance the radiation sensitivity in cancer cells but not in nonmalignant breast cells, though both cell lines uptook the same level of Glu-AuNPs.

pH-responsive gold nano-materials provide an alternate mechanism for drug release, taking advantage of the acidic condition inside tumor and inflamed tissues (pH=6.8) and cellular compartments, including endosomes (pH=5.56) and lysosomes (pH=4.55.0) [122].

Schoenfisch et al. [123] have likewise shown that nitric oxide [NO] can be efficiently released at acidic pH from gold nanoparticles.

Recent studies [124] have established that nanoparticles are able to release localized X-rays when activated with a high energy proton beam by particle-induced X-ray emission effect, leading to an increase in low energy X-ray emission from the tumor itself and, potentially, to an increase in the dose absorbed within the tumor cells. These investigations support the hypothesis that dose absorption, and thus the relative biological effectiveness of proton radiotherapy, can be enhanced by delivering targeted gold nanoparticles to a tumor prior to treatment. Moreover, it has been demonstrated that both the

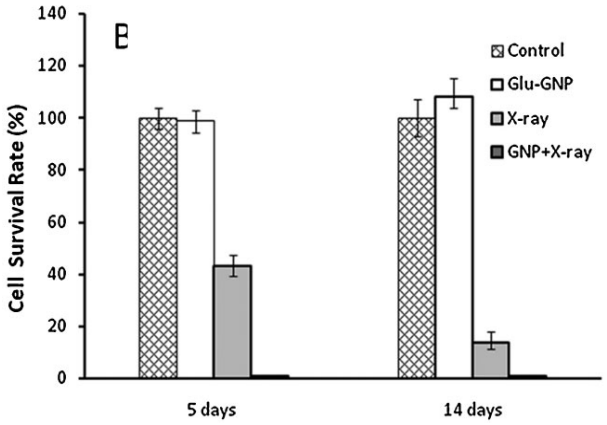

Fig. 9 Cell survival rate of MCF-7 breast-cancer cells induced by 200 kVp X-ray irradiation with or without gold nanoparticle, is determined by clonogenic survival assay (at 5 days and 14 days). Adapted with permission from Reference [121]. Copyright 2008 Wiley-VCH Verlag GmbH Co.

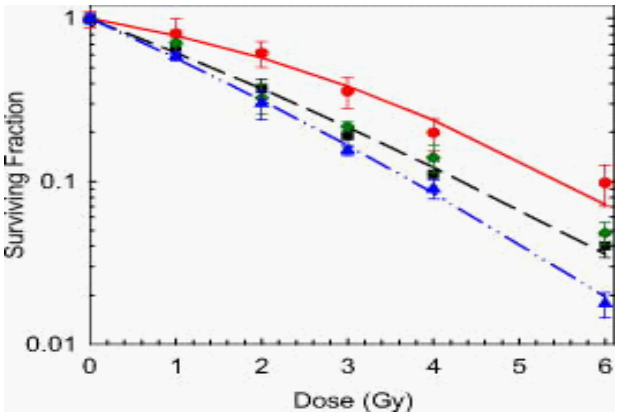

Fig. 10 Cell survival as a function of dose for untreated cells irradiated with ^{60}Co (circles) and proton (squares) beams, as well as for phage-only (diamonds) and Au-treated (triangles) cells irradiated with protons. Errors bars represent one-sigma standard deviation of the mean of the six samples irradiated for each dose. Redrawn with permission from Reference [125].

size and the amount of particle uptake into cells affect the radiosensitization, resulting in a new treatment option for infiltrative tumors and other diffusive inflammatory diseases.

Polf et al. [125] quantified enhancements of cell death and relative biological effectiveness for human prostate carcinoma cells that contain internalized gold nanoparticles, over a range of clinically relevant doses. Typical results are summarized in Fig. 10 that shows an increase of efficacy of the proton beam therapy of prostate cancer by more than 20%.[125], compared with untreated cells irradiated with ^{60}Co. These authors [125] interpreted these results as an indication of increased ionization density within the cells, resulting from interactions between the proton beam and internalized gold nanoparticles. These ionizations lead to increased production of low-energy δ-ray electrons which produce a high degree of lethal damage within the cells.

Finally, it must be mentioned that gold nanoparticles can also exhibit intrinsic anticancer properties. Many works have clearly demonstrated that gold nanoparticles are able to alter the cell cycle, including cell division, signaling and proliferation and these particles can be used as cancer-selective cytotoxic agent. For example, changes in cell cycle in radiation-resistent human prostate carcinoma cell line were produced by a treatment *in vitro* with glucose-capped gold nanoparticles (Glu-AuNPs, ca. 10 nm in size) [126], able to arrest the cancer cells in the G2/M phase of the cell cycle. Glu-AuNPs trigger activation of the CKD kinases leading to cell cycle acceleration in the G0/G1 phase and accumulation in G2/M phase. This activation is accompanied by a striking sensitization to ionizing radiation. This result suggests that this treatment is expected to increase the efficacy of a subsequent radiotherapy action.

In another example, gold nanoparticles targeted to nuclei by properly conjugation with specific peptides, induce DNA damage, cytokinesis arrest and apoptosis in malignant cells, as revealed by confocal microscopy images, showing that localization of gold nanoparticles at the nucleus of a cancer cell damages the DNA [127].

Clinical studies have ascertained that tumor necrosis factor [TNF], a cytokine that has shown antitumor properties, can be delivered to the target tissue through its complexation with gold nanoparticles. TNF is able to significantly increase the permeability of the tumor vasculature, causing destruction of the vascular lining and allowing for greater delivery of other chemotherapeutic drugs [128,129]. Moreover, TNF conjugation to gold nanoparticles reduces its toxicity allowing for significantly higher dosages to be delivered to the tumor cells.

3.3 Cell membrane penetration and delivery pathways.

Although most gold nanoparticle conjugates exhibit some degrees of intracellular permeation, the intracellular fate and cellular uptake depend critically, as we have above stated, on their charge, size, lipophilicity and surface functionality. Typically, AuNPs administrated intravenously are mostly taken up by the liver and the spleen and the amount of particles accumulated in different organs differs substantially, depending on their geometry [81,130]. As a significant example, in Fig. 11, we show typical results of biodistribution of gold nanoparticles after intravenous injection into mice, where the effect of the different

geometries is clearly evidenced.

Among others, nanoparticle size is the main parameter affecting the cellular uptake rate, influencing their internalization mechanism [131]. Yu Pan et al. [132] compared interactions of AuNPs (size from 0.8 up to 15 nm) with various cell types, representing the principal barriers and lining cells of the body (epithelial and endothelial cells), phagocytes (macrophages), and tissue stromal cells (connective tissue fibroblasts). Their results suggest different uptake kinetics and/or cellular target specificities, even for similarly sized gold nanoparticles. Hillyer et al. [133] showed that, after oral administration of AuNPs (58, 28, 10 and 4 nm in size) to mice, an increased distribution to other organs was observed, in particular the smallest particles (4 nm) were found in kidney, liver, spleen, lungs and even in the brain.

A systematic study by De Jong et al. [134] has undoubtedly demonstrated that gold nanoparticles preferably accumulate in organs in a size dependent manner. Gold nanoparticles 10 nm in size accumulated in kidney, testis, thymus, heart, brain, spleen and liver, while particles 50 nm in size accumulate preferentially in lung, spleen and liver, and particles with size larger than 100 nm accumulated in spleen and liver exclusively. Similarly, Chan et al. [135] have reported cellular uptake that is likewise dependent on the size of nanoparticles.

In the following, we highlight selected systems that illustrate how the chemical structure of the NP surface functionality can be used to regulate cell uptake and particle distribution in tissues. In addition, the surface charge of nanoparticles can contribute to enhance their ability to respond to external or internal stimuli [136,137].

To overcome the problem connected with the penetration of the cell membrane and the permeation into the cytosol, nanoparticles can be coated with cell penetrating peptides, such as peptides containing the amino acid sequence Arg-Gly-Asp [RGD] [138], insect neuropeptide, namely, allatostatin 1 from Drosophila melanogaster [139], poly(L-lysine) [PLL] [140] and and arginine-rich peptides (CALNN and its derivatives) [141]. In fact, peptide coated nanoparticles were found to have favorable characteristics, including small particle size, near-neutral ζ-potential, and stability in serum. Moreover, at appropriate formulation, the coated nanoparticles enable effective ligand-specific gene delivery to human primary endothelial cells in serum-containing media.

Nativo et al. [78] investigated, by means of transmission electron microscopy (TEM) measurements, the uptake of surface-modified gold nanoparticles (16 nm in size) by human fibroblast cells (HeLa cells). They clearly demonstrated that the well-established endosomal route of cellular uptake can be bypassed by controlling the uptake mechanism by nanoparticle surface modification with so-called cell penetrating peptides (CPPs).

In a similar study, Kang et al. [127] reported that gold NPs, 30 nm in size, coated with poly-ethylene glycol [PEG] and conjugated with an arginine-glycine-aspartic acid peptide [RDG] and a nuclear localization agent [NLS] peptide can penetrate to the nucleus after endosomal escape and induce DNA damage in cancer cells. From a basic point of view, these results show that gold nanoparticles localized at the nucleus of cancer cells have important implications in understanding the interactions between nanomaterials and living systems.

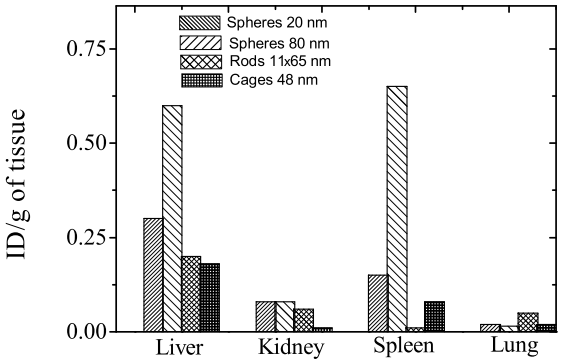

Fig. 11 Biodistribution of gold particles with different geometries. The sizes of nanospheres, nanorods and nanocages are labeled as diameter, width x length and outer edge lenght, respectively. The figure was re-plotted with permission from Reference [142]

Rotello and Vachet [143,144] have shown that electrical surface charge and hydrophobicity contribute to determine the cellular uptake of functionalized AuNPs. The surface charge of the AuNPs is a key parameter for nanoparticle-cell membrane interaction and subsequent intracellular internalization. In general, cationic NPs, due to electrostatic attraction, interact more strongly with the cell membrane due to the presence of negatively charged groups (e.g., sialic acid) onto cellular membranes, and hence show higher uptake efficiency compared to their anionic and neutral counterparts. In these studies [143,144], AuNPs ranging in size from 2-100 nm were coated with Herceptin and were tested for breast cell internalization mediated by the ErbB2 receptor. The most efficient cellular uptake was observed by Zhu et al. [143,144] with particles ranging from 20÷50 nm. Apoptosis was also enhanced by 40÷50 nm gold nanoparticles. *In-vivo* studies of passive targeting of tumors was also performed with AuNPs ranging from 10÷100 nm. These authors [143,144] found smaller AuNPs rapidly diffused into the tumor matrix, whereas larger AuNPs stayed near the vasculature. It must be noted, however, that strong electrostatic attraction can result in significant cytotoxicity, due to partial membrane disruption.

Stellacci et al. [145] found that ligand shell morphology af-

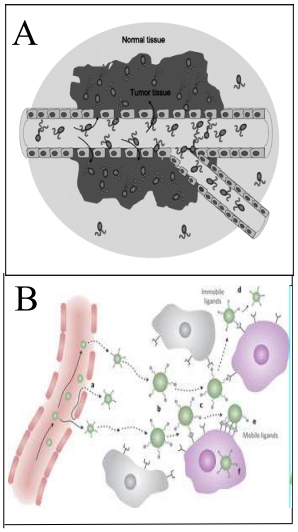

Fig. 12 Drug-loaded gold nanoparticles carrying therapeutics to tumor sites through extravasation from leaky tumor vessels. Panel A): passive targeting (Adapted and reproduced with permission from Reference [148]). Panel B): active targeting (Adapted and reproduced with permission from Reference [149]).

fects cell membrane penetration of AuNPs. It was shown that AuNPs with structured ligand shells could directly pass through the plasma membrane of cells without the creation of pores. Surface modifications to the ligand shell allow for targeting of specific organelles. Brust et al.[146] utilized transmission electron microscopy to demonstrate that, modifying the AuNP surface with cell penetrating peptides, the nucleus and other organelles could be specifically targeted. In particular, peptide-capped NPs with different recognition motifs have been successfully employed by Nativo et al.[78] using surface modification based on different cell-penetrating peptides and a peptide acting as a nuclear localization signal.

Feldheim et al.[147] have also shown nuclear targeting of AuNPs by modifying the surface with a nuclear localization sequence. These authors employed five peptide-nanoparticle complexes to target the nucleus of HepG2 cells. The particle conjugates were formulated in different ways, using nuclear localization signal [NLS] from SV40 virus, the adenovirus [NLS], the adenovirus receptor-mediated endocytosis [RME] peptide, a long peptide containing the adenovirus RME and NLS peptides and, finally, the adenovirus RME and NLS peptides attached to nanopartcles as separate pieces. In spite of the different formulations, all the conjugates were able to target the nucleus of the cells. These researches highlight the perspectives that AuNP bioconjugates are expected to fulfill in the future of nanomedicine.

A final comment on the delivery mechanisms of gold nanoparticles in the case of intravenous injection is in order. After administration into the circulatory system, gold nanoparticle targeting occurs through two different, hereafter reported, mechanisms, which take advantage of the fact that, thanks to angiogenesis and neo-vascularization, blood vessels are scattered with numerous gaps, big enough for nano-carriers to leak out into the tumor.

Indeed, the accumulation mechanism of intravenously injected AuNPs relies on passive targeting diffusion, based on the homing of carriers by simple diffusion from leaky blood vessel due to the defective vascular architecture in the cancerous tissues (and coupled with a poor lymphatic drainage).[148,150]. On the other hand, active targeting, presenting ligands (peptides or poteins) on the gold particle surface for specific recognition by cell surface receptors, increases the probability to bind to specific molecules on the targeted cells. Fig. 12 shows a cartoon of the gaps in vessels allowing nanoparticles to enter by passive and active targeting.

Gold nanoparticles are particularly suitable for *in vivo* applications to reach the diseased tissues through administration into the circulatory system, since their small size and their hydrophilic surface can prevent their uptake by the mononuclear phagocyte system, reducing opsonization reactions and subsequent clearance by macrophages[151,152].

4 Gold nanoparticle toxicity.

Toxicity of AuNPs is a crucial issue that can limit their biomedical applications. Prior to an extensive clinical use, the whole body effect of gold nanoparticles must be, of course, accurately assessed. It remains an important and urgent task to evaluate the possible toxicity compared with the overall health benefit.

Based on a wide experimental investigation, such as viability assay, reactive oxygen species analysis, gene expression- and cellular morphology assay, gold nanoparticles, in contrast to silver nanoparticles, are considered fairly non-toxic[153,154], even if the capping agents may change the toxic profile. However, caution should be required since gold nanoparticles are light absorbers in the visible region and consequently colorimetric and fluorescence assays could result altered[155]. A comprehensive analysis of how AuNPs can influence a living organism through different biological pathways can be found in the review by Nel et al.[156].

The cytotoxicity of gold nanoparticles in human cells has been studied in detail, and the results have shown that 18 nm in size nanoparticle preparations with citrate and biotin surface modifiers did not appear to be toxic at concentrations up to 250 μM. In contrast, the gold-salt precursor ($AuCl_4^-$) solution was over 90% toxic at a concentration of 200 μM. The nanoparticle preparations with glucose or cysteine sur-

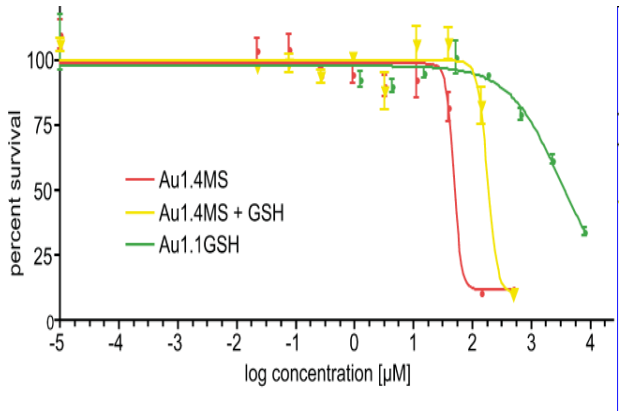

Fig. 13 IC_{50} of AuNP- and Au1.1GSH-treated HeLa cells. Au1.1GSH (green, IC_{50}=3130 μM) has a 65-fold higher IC_{50} than Au1.4MS (red, IC_{50}=48 μM). The IC_{50} of Au1.4MS admixed with 10 equivalents of GSH is intermediate at 181 μM. Adapted with permission from Reference [158] copyright 2009 Wiley-VCH Verlag GmbH Co.

face modifiers were not toxic at concentration up to 25 μM. In these experiments, nanoparticles were tested for cytotoxicity using the K562 leukemia cell line [157].

For example, Wang et al. [154] found that the oxidation states of gold did not change even after long-term retention in the liver and spleen in rats intra venous injected with gold nanorods (55.6 nm length and 13.3 nm width), as revealed by combination of transmission electron microscopy and X-ray absorption spectra.

About the *in vivo* toxicity of AuNPs, most researchers did not find any toxicological effects in the various animal models. As an example, Pokharkar et al. [159] found that the median lethal dose (LD_{50}) value of chitosan-coated AuNPs was greater than 2000 μg/kg after oral administration in rats. In the case of sub-acute oral toxicity studies, the chitosan- coated AuNPs were orally administrated to male and female rats for a period of 28 days. All the animals survived for the duration of the study, with no significant changes in clinical signs, body weight, food consumption, hematological parameters, organ weights, and no histopathological observations were found.

However, different effects have been evidenced, based on *in vitro* cellular assay. Among them, it deserves to be mentioned those reported in a detailed study carried out by Pan et al. [158] on the cellular response toward exposure to AuNPs (1.4 nm in size) capped with triphenylphosphine monosulfonate [TPPMS]. Cells internalized the particles and mounted a robust stress response on the level of membrane and mitochondria integrity and messenger RNA (mRNA) induction. In this case, cell death suggested strong oxidative damage and mitochondrial permeability transition as the prime cause of cell death, producing reactive oxygen species. Fig. 13 clearly shows the behavior of AuNPs treated with triphenylphosphine monosulfonate [TPPMS] (AuMS, 1.4 nm in size) compared with AuNPs treated with glutathione ligand (AuGSH, 1.1 nm in size). As can be seen, the IC_{50} of AuGSH was 3130 μM (green curve), 65-fold higher than the IC_{50} of AuMS, which was 48 μM (red curve). When AuMS and AuGSH (10 equiv) were mixed and the mixture added to the cells (yellow curve), the IC_{50} of the mixture was 181 μM and thus almost fourfold higher than that of AuMS alone.

The authors propose that the toxicity of small AuNPs depends on their ability to trigger the intracellular formation of reactive oxygen species [ROS] from dioxygen. In addition, the different cell response to the various AuNP coatings might also reflect a different uptake propensity. The cellular responses observed after AuNP exposure indicated a strong oxidative stress response that exacerbated cellular ROS. The fact that antioxidants reduced toxicity and that the cells executed a strong genomic stress response supports this concept. From these results, these authors [158] concluded that Au1.4MS nanoparticles induced oxidation stress and triggered cell death by necrosis.

Finally, numerous studies evidenced that size, as well as the electrical charge of the nanoparticles, play a significant role in cytotoxicity and geno-toxicity. In particular, charged AuNPs induce apoptosis and neutral AuNPs induce necrosis [160].

Among other parameters, the route of administration influences the pharmacokinetics, biodistribution and toxicity profile of gold nanoparticles. A comprehensive survey of this important feature is reported in the review by Arvizo et al. [161] who summarized the toxicology profile of different formulated nanoparticles in dependence on their mode of administration. A summary of the biodistribution and toxicity of AuNPs in different animal models is also provided by Li and Chen [162]. Regarding the biodistribution, one can see that, regardless of the animal model, dosage, size, and coating of the AuNPs, the targeted tissues after AuNPs exposure are mainly the liver and spleen, which are part of the immune system and involved in the uptake and metabolism of exogenous molecules. As a partial conclusion, one can assert that the majority of gold particles was detected in the livers and spleens for all sizes. Moreover, tissue distribution of AuNPs resulted size-dependent, with the smallest (10 nm in size) nanoparticles having the most widespread organ distribution.

In most cases, as we have already stated, toxicity depends on the dose and at present there is no standard dose known as safe or conversely known as toxic.

Finally, it deserves to be mentioned here that the *purity* of gold formulation can play a role in the toxicological investigations. For example, free surfactants and metal ions present in the solution, rather than gold particles, could determine toxicity [163]. A combined effort by nanotechnology researchers and

biologists as a fruitful approach is necessary to reach definitive conclusions regarding the toxicity of gold nanoparticles.

5 Conclusions

Gold nanoparticles, owing to the rapid development of the technologies for their chemical synthesis and their characteristics such as stability, tunable surface monolayers, functional flexibility and low toxicity, are promising new vehicles for drug and gene delivery. Their diverse functionalities allow to fulfill a variety of aims that can be achieved by tuning size, shape, structure and optical properties. A series a different approaches, offering opportunities in anti-cancer treatments and involving photothermal therapy, drug delivery, gene therapy and cell cycle regulation, have been investigated so far.

However, although a lot of investigations remains to be done and, to date, the physiological destination of nanoparticles *in vivo* is still far from completely understood, nanoparticles definitely have the potential to revolutionize medical therapies, particularly in the case of cancer multimodal treatment.

More investigations are still needed to get a better understanding of how we can extrapolate the potential effects on human health from their biological behavior observed in animal studies, and how characteristics and properties of these nanoparticles influence their fate and behavior *in vivo*.

In this review, we have presented a summary of the most recent applications of functionalized gold nanoparticles considered as extraordinary molecular carriers for the targeting, intracellular trafficking and delivery of a huge array of biomolecules and other molecules of biological and therapeutical relevance.

6 Acknowledgements

We acknowledge support by grants from Ateneo Sapienza 2011/C26A11PKS2 and 2013/C26A13HRZ4. This work has been partially supported by the Dipartimento di Chimica, "Sapienza" *Università di Roma* through the "Supporting Research Initiative 2013".

References

1 E. Boisselier and D. Astruc, *Chem. Soc. Rev.*, 2009, **38**, 1759–1782.
2 C. M. Cobley, J. Chen, E. C. Cho, L. V. Wang and Y. Xia, *Chem. Soc. Rev.*, 2011, **40**, 44–56.
3 D. L. and N. Khlebtsov, *Che. Soc. Rev.*, 2009, **38**, 1759–1782.
4 C. J. Murphy, A. M. Gole, J. W. Stone, P. N. Sisco, A. M. Alkilany, E. C. Goldsmith and S. C. Baxter, *Acc. Chem. Res.*, 2008, **41**, 1721–1730.
5 G. F. Paciotti, D. G. I. Kinkston and L. Tamarkin, *Drug. Dev. Res.*, 2006, **5**, 2255–2262.
6 B. Duncan, C. Kim and V. M. Rotello, *J. Control. Release*, 2010, **148**, 122–127.
7 C. Brigger, C. Dubernet and P. Couvreur, *Adv. Drug Delivery Res.*, 2012, **64**, 24–36.
8 I. Fratoddi, I. Venditti, C. Cametti, C. Palocci, L. Chronopoulou, M. Marino, F. Acconcia and M. V. Russo, *Colloids Surfaces B: Biointerfaces*, 2012, **93**, 59–66.
9 I. Venditti, I. Fratoddi, C. Battocchio, G. Polzonetti, C. Cametti and M. V. Russo, *Polymer International*, 2011, **60**, 1222–1229.
10 A. Lagana, I. Venditti, I. Fratoddi, A. L. Capriotti, G. Caruso, C. Battocchio, G. Polzonetti, F. Acconcia, M. Marino and M. V. Russo, *J. Colloid Interface Sci.*, 2011, **361**, 465–471.
11 E. S. Bronze-Uhle, A. Batagin-Neto, D. M. Fernandes, I. Fratoddi, M. V. Russo and C. F. O. Graeff, *Appl. Phys. Lett.*, 2013, **102**, 241917–4pp.
12 I. Fratoddi, E. S. Bronze-Uhle, M. V. Russo, G. Polzonetti and C. F. O. Graeff, *J. Phys. Chem. A*, 2012, **116**, 8768–8774.
13 I. Venditti, I. Fratoddi, M. V. Russo and A. Bearzotti, *Nanotechnology*, 2013, **24**, 155503–.
14 A. G. Skirtach, A. M. Javier, O. Kreft, K. Kolher, A. P. Alberola, H. Mohwald, W. J. Parak and G. B. Sukhorukov, *Angew. Chem.*, 2006, **118**, 4728–4733.
15 S. R. Sershen, S. L. Westcott, N. J. Halas and J. L. West, *J. Biomed. Mater. Res.*, 2000, **51**, 293–298.
16 R. Sardar, A. M. Funston, P. Mulvaney and R. W. Murray, *Langmuir*, 2009, **25**, 13840–13851.
17 M. De, P. S. Ghosh and V. M. Rotello, *Adv. Materials*, 2008, **20**, 4225–4241.
18 *Gold nanoparticles: properies, characterization and fabrication*, ed. E. P. Chow, Nova Science Publisher, New York, 2010.
19 R. Wilson, *Chem. Soc. Rev.*, 2008, **37**, 2028–2045.
20 *Gold: Science and applications*, ed. C. Corti and R. Holliday, CRC Press, Boca Raton, 2010.
21 Y. Niidome, T. Niitidome, S. Yamada, Y. Horiguchi, H. Takahashi and K. Nahashima, *Mol. Cryst. Liq. Cryst.*, 2006, **445**, 201–206.
22 D. Pissuwan, T. Niidome and M. B. Cortie, *J. Control Release*, 2011, **149**, 65–71.
23 A. J. Mieszawska, W. J. M. Mudler, Z. A. Fayad and D. P. Cormode, *Mol. Pharmaceutics*, 2013, **10**, 831–847.
24 P. Zhao, N. Li and D. Astruc, *Chemistry Rev.*, 2013, **257**, 638–665.
25 I. Fratoddi, I. Venditti, C. Battocchio, G. Polzonetti, F. Bondino, M. Malvestuto, E. Piscopiello, L. Tapfer and M. V. Russo, *J. Phys. Chem. C*, 2011, **115**, 15198–15204.
26 C. Battocchio, C. Meneghini, I. Fratoddi, I. Venditti, M. V. Russo, G. Aquilanti, C. Maurizio, F. Bondino, R. Matassa, M. Rossi, S. Mobilio and G. Polzonetti, *J. Phys. Chem. C*, 2012, **116**, 19571–19578.
27 R. Matassa, I. Fratoddi, M. Rossi, C. Battocchio, R. Caminiti and M. V. Russo, *J. Phys. Chem. C*, 2012, **116**, 15795–15800.
28 C. Cametti, I. Fratoddi, I. Venditti and M. V. Russo, *Langmuir*, 2011, **27**, 7084–7090.
29 I. Fratoddi, C. Battocchio, G. Polzonetti, F. Sciubba, M. Delfini and M. V. Russo, *Eur. J. Inorganic Chem.*, 2011, **31**, 4906–4913.
30 I. Fratoddi, I. Venditti, C. Battocchio, G. Polzonetti, C. Cametti and M. V. Russo, *Nanoscale Res. Lett.*, 2011, **6**, 98–106.
31 F. Vitale, I. Fratoddi, C. Battocchio, E. Piscopiello, L. Tapfer, M. V. Russo, G. Polzonetti and C. Giannini, *Nanoscale Res. Lett.*, 2011, **6**, 103–112.
32 P. M. Tiwari, V. K., V. A. Dennis and S. R. Singh, *Nanomaterials*, 2011, **1**, 31–63.
33 P. S. De, M. Ghosh and V. M. Rotello, *Advanced Materials*, 2008, **20**, 4225–4241.
34 G. D. Khan, G. D. Vishakante and H. Siddaramaiah, *Adv. Colloid Interface Sci.*, 2013, **199-200**, 44–58.
35 C. H. Chou, C. D. Chen and C. Wang, *J. Phys. Chem. B*, 2005, **109**, 11135–11138.

36 I. H. El-Sayed, X. Huang and M. A. El-Sayed, *Cancer Lett.*, 2006, **239**, 129–135.

37 D. P. O'Neil, L. R. Hirsch, N. J. Halas, J. D. Payne and L. J. West, *Cancer Lett.*, 2004, **209**, 171–176.

38 R. Weissleder, *Nature Biotech.*, 2009, **19**, 316–317.

39 X. Xu and M. Cortie, *Advanced Functional Materials*, 2006, **16**, 2170–2176.

40 *Electrochemical methods: undamentals and Applications*, ed. A. J. Bard and L. R. Faulkner, John Wiley, New York, 2nd edn, 2001.

41 E. C. Dreaden, A. M. Alkilany, X. Huang, C. Murphy and M. A. El-Sayed, *Chem. Soc. Rev.*, 2012, **41**, 2740–2779.

42 A. M. Alkilany, R. L. Frey, J. L. Ferry and C. j. Murphy, *Langmuir*, 2008, **24**, 10235–10239.

43 C. K. Kim, P. Ghosh, C. Pagliuca, Z. J. Zhu, S. Menichetti and V. M. Rotello, *J. Am. Chem. Soc.*, 2009, **131**, 1360–1361.

44 L. Chen and H. A. Klok, *Soft Matter*, 2013, **9**, 10678–10688.

45 S. T. Guo, Y. Y. Huang, Q. A. Jiang, Y. Sim, D. L. Deng, Z. C. Liang, Q. A. Du, J. F. Xing, Y. L. Zhao, P. C. Wang, A. J. Dong and X. L. Liang, *ACS Nano*, 2010, **4**, 5505–5511.

46 C. Boyer, M. R. Whittaker, K. Chuad, J. Liu and T. P. Davis, *Langmuir*, 2010, **26**, 2721–2730.

47 C. Boyer, V. Bulmus, P. Davis Thomas, V. Ladmiral, J. Liu and S. Perrier, *Chem. Rev.*, 2009, **109**, 5402–5436.

48 C. Boyer, M. Whittaker, M. Luzon and T. P. Davis, *Macromolecules*, 2009, **42**, 6917–6926.

49 H. Takahashi, T. Niidome, A. Nariai, Y. Niidome and S. Yamada, *Nanotechnology*, 2006, **17**, 4431–4435.

50 Y. Cheng, A. C. Samia, J. Li, M. Kenney, A. Resnik and C. Burda, *Langmuir*, 2010, **26**, 2248–2255.

51 Y. Cheng, J. D. Meyers, A. M. Broome, M. Kenney, J. Basilion and C. Burda, *J. Am. Chem. Soc.*, 2011, **133**, 2583–2591.

52 G. J. Higby, *Gold Bull.*, 1982, **15**, 130–140.

53 D. A. Rosi, N. L.and Giljohann, C. S. Thaxton, A. K. R. Lytton-Jean, M. S. Han and C. A. Mirkin, *Science*, 2006, **312**, 1027–1030.

54 L. Poon, W. Zandberg, D. Hsiao, Z. Erno, D. Sen, D. B. Gates and N. R. Branda, *ACS Nano*, 2010, **4**, 6395–6403.

55 K. Kneipp, Y. Wang, H. Kneipp, L. T. Perelman, I. Itzkan, R. R. Dasari and M. S. Feld, *Phys. Rev. Lett.*, 1997, **78**, 1667–1670.

56 X. Qian, X. H. Peng, D. O. Ansari, Q. Yin-Goen, G. Z. Chen, D. M. Shin, L. Yang, A. N. Young, M. D. Wang and S. Nie, *Nat. Biotechnol.*, 2008, **26**, 83–90.

57 E. Oh, K. Susuke, A. J. Markinen, J. R. Deschamps, A. L. Huston and I. L. Medintz, *J. Chem. Phys. C*, 2013, **117**, 18947–18956.

58 D. Shenoy, W. Fu, J. Li, C. Crasto, G. Jones, C. Di Marzio, S. Sridhar and M. Amiji, *Int. J. Nanomedicine*, 2006, **1**, 51–57.

59 S. D. Brown, P. Nativo, J. A. Smith, P. Stirling, P. R. Edwards, B. Venugopal, D. J. Flint, J. A. Plumb, D. Graham and N. J. Wheate, *J. Am. Chem. Soc.*, 2010, **132**, 4678–4684.

60 S. Dhar, W. L. Daniel, D. A. Giljoham, C. A. Mirkin and S. J. Lippard, *J. Am. Chem. Soc.*, 2009, **131**, 14652–14653.

61 S. D. Brown, P. Nativo, J. A. Smith, D. Stirling, P. R. Edwards, B. Venugopal, D. J. Flint, J. A. Plumb, D. Graham and N. J. Wheate, *J. Am. Chem. Soc.*, 2010, **132**, 4678–4684.

62 A. R. Rothrock, R. L. Donkers and M. H. Schoenfisch, *J. Am. Chem. Soc.*, 2005, **127**, 9362–9363.

63 M. A. Polizi, N. A. Stasko and M. H. Schoenfisch, *Langmuir*, 2007, **23**, 4938–4943.

64 S. S. Agasti, A. Chompoosor, C. C. You, P. Ghosh, C. K. Kim and V. M. Rotello, *J. Am. Chem. Soc.*, 2009, **131**, 5728–5729.

65 M. S. Yavuz, Y. Cheng, C. M. Cobley, Q. Zhang, M. Rycenga, J. Xie, C. Kim, K. H. Song, A. G. Schwartz, L. V. Wang and Y. Xia, *Nature Materials*, 2009, **9**, 935–939.

66 D. G. Moon, S. W. Choi, X. Cai, W. Y. Li, E. C. Cho, U. Jeong, L. V. Wang and Y. A. Xia, *J. Am. Chem. Soc.*, 2011, **133**, 4762–4765.

67 J. You, G. Zhang and C. Li, *ACS Nano*, 2010, **4**, 1033–1041.

68 A. Verma and V. M. Rotello, *Chem. Comm.*, 2005, 303–312.

69 C. M. McIntosh, E. A. Esposito, A. K. Boal, J. M. Simard, C. T. Martin and V. M. Rotello, *J. Am. Chem. Soc.*, 2001, **123**, 7626–7629.

70 P. S. Ghosh, C. K. Kim, G. Han, N. S. Forbes and V. M. Rotello, *ACS Nano*, 2008, **2**, 2213–2218.

71 I. Andre, S. Linse and F. A. A. Mulder, *J. Am. Chem. Soc.*, 2007, **129**, 15805–15813.

72 H. C. Huang, S. Barua, D. B. Kay and K. Rege, *ACS Nano*, 2009, **3**, 2941–2952.

73 W. Cai, T. Gao, H. Hong and J. Sun, *Nanothechn. Sci. Appl.*, 2008, **1**, 17–32.

74 E. C. Cho, J. Xie, P. A. Wurm and Y. Xia, *Nano Lett.*, 2009, **9**, 1080–1084.

75 A. Chompoosor, G. Han and V. M. Rotello, *Biocojugate Chem.*, 2008, **19**, 1342–1345.

76 W. Jiang, Y. S. KimBetty, J. T. Rutka and C. W. Chanwarren, *Nature Nanotechnology*, 2008, **3**, 145–150.

77 A. Verma, O. Uzun, Y. Hu, H. S. Han, N. Watson, S. Chen, D. J. Irvine and F. Stellacci, *Nature Materials*, 2008, **7**, 588–595.

78 P. Nativo, I. A. Prior and M. Brust, *ACS Nano*, 2008, **2**, 1639–1644.

79 Y. S. Chen, Y. C. Hung, I. Liau and G. S. Huang, *Nanoscale Res. Lett.*, 2009, **4**, 858–864.

80 S. D. Perrault, C. Walkey, T. Jennings, H. C. Fischer and W. C. W. Chan, *Nano Lett.*, 2009, **9**, 1909–1915.

81 G. Zhang, Z. Yang, W. Lu, R. Zhang, Q. Huang, M. Tian, L. Li, D. Liang and C. Li, *Biomaterials*, 2009, **30**, 1928–1936.

82 L. Balogh, S. S. Nugavekar, B. M. Nair, W. Lesniak, C. Zhang, S. L. Y., M. S. T. Kariapper, A. El-Jawahri, M. LLanes, B. Bolton, F. Mamou, W. Tan, A. Hutson, L. Minc and M. K. Khan, *Nanomed.: Nanothechol. Biol. Med.*, 2007, **3**, 281–296.

83 S. Hirn, M. Semmler-Behnke, C. Schleh, A. Wenk, J. Lipka, M. Schaffer, S. Takenaka, W. Moller, G. Schmid, U. Simon and W. G. Kreyling, *Eur. J. Pharm. Biopharm.*, 2011, **77**, 407–416.

84 G. Sonavane, K. Tomoda, A. Sano, H. Ohshima, H. Terada and M. Makino, *Colloids Surfaces B*, 2008, **65**, 1–10.

85 G. Han, C. T. Martin and V. M. Rotello, *Chem. Biol. Drug Des.*, 2006, **67**, 78–82.

86 G. Han, N. S. Chari, A. Verma, R. Hong, C. T. Martin and V. M. Rotello, *Bioconjug. Chem.*, 2005, **16**, 1356–1359.

87 M. Oishi, J. Nakaogami, T. Ishii and Y. Nagasaki, *Chem. Lett.*, 2006, **35**, 1046–1047.

88 T. Niidome, K. Nakashima, H. Takahashi and Y. Niidome, *Chem. Commun.*, 2004, 1978–1979.

89 Y. Niidome, T. Niitidome, S. Yamada, Y. Horiguchi, H. Takahashi and K. Nahashima, *Mol. Cryst. Liq. Cryst.*, 2006, **445**, 491–496.

90 A. Wijaya, S. B. Shaffer, I. G. Palleres and K. Hamad-Schifferli, *ACS Nano*, 2008, **3**, 80–86.

91 T. Kawano, M. Yamagata, H. Takahashi, Y. Niidome, S. Yamada, Y. Katayama and T. Niidome, *J. Control Release*, 2006, **111**, 382–389.

92 S. M. Noh, W. Kim, S. J. Kim, J. M. Kim, K. H. Baek and Y. K. Oh, *Biochim. Biophys. Acta*, 2007, **1770**, 747–752.

93 T. Tencomnao, A. Apijaraskul, V. Rakkhithawatthana, S. Chaleawlert-umpon, N. Pimpa, W. Sajomsang and N. Saengkrit, *Charbohydr. Polym.*, 2011, **84**, 216–222.

94 J. A. Fortune, T. I. Novobrantseva and A. M. Klibanov, *J. Drug Delivery*, 2011, **2011**, 204058.

95 L. Z. Feng, S. Zhang and Z. Liu, *Nanoscale*, 2011, **3**, 1252–1257.

96 C. Xu, D. Yang, L. Mei, B. Lu, Q. Li, H. Zhu and T. Wang, *ACS Applied Mat. Interfaces*, 2013, **5**, 2715–2724.

97 S. Lal, S. E. Clare and N. J. Halas, *Acc. Chem. Res.*, 2008, **41**, 1842–1851.

98 X. Huang, I. H. El-Sayed, W. Qian and M. A. El-Sayed, *J. Am. Chem. Soc.*, 2006, **128**, 2115–2120.

99 F. Ren, S. Bhana, D. D. Norman, J. Johnson, L. Xu, D. L. Boker, A. L. Parvill and X. Huang, *Bioconuigate Chem.*, 2013, **24**, 376–386.

100 L. Tong, Y. Zhao, T. B. Huff, M. W. Hansen, A. Wei and J. X. Cheng, *Adv. Mat.*, 2007, **19**, 3136–3146.

101 J. Chen, D. Wang, J. Xi, L. Au, A. Seikkinen, A. Warsen, Z. Y. Li, H. Zhang, Y. Xia and X. Li, *Nano Lett.*, 2007, **7**, 1318–1322.

102 L. R. Hirsch, R. J. Stafford, J. A. Bankson, S. R. Sershen, B. Rivera, R. E. Price, J. D. Hazle, N. J. Halas and J. L. West, *Proc. Natl. Acad. Sci.*, 2003, **100**, 13549–13554.

103 J. M. Stern, J. Stanfield, Y. Lotan, S. Park, J. T. Hsieh and J. A. Cadeddu, *J. Endourol.*, 2007, **21**, 939–943.

104 J. M. Stern, J. Stanfield, W. Kabbani, J. T. Hsieh and J. A. Cadeddu, *J. Urol.*, 2004, **209**, 171–176.

105 H. Maeda, J. Wu, T. Sawa, Y. Matsumura and K. Hori, *J. Control Release*, 2000, **65**, 271–284.

106 V. Raji, J. Kumar, C. S. Rejina, M. Vibin, V. N. Shenoi and A. Abraham, *Exp. Cell. Res.*, 2011, **317**, 2052–2058.

107 M. A. Zaki, S. Akhter, Z. Rahman, M. Anwwar, N. Mallik and F. J. Ahmad, *J. Pharm. Pharmacol.*, 2013, **65**, 634–642.

108 E. Bonaiuto, A. Milelli, G. Cozza, V. Tumiatti, C. Marchetti, E. Agostinelli, C. Fimognari, P. Hrelia, A. Minarini and M. L. Di Paolo, *Europ. J. Med. Chem.*, 2013, **70**, 88–101.

109 M. Chamundeeswari, T. P. Sastry, B. S. Lakhsmi, V. Senthil and E. Agostinelli, *Biochim. Biophys. Acta*, 2013, **1830**, 3005–3010.

110 C. Loo, A. Lin, L. Hirsch, M. H. Lee, J. Barton, N. Hals, J. West and R. Drezek, *Techn. Cancer Res. Treat.*, 2004, **3**, 33–40.

111 V. P. Zharov and V. Galitovsky, *Appl. Phys. Lett.*, 2003, **83**, 4897–4899.

112 K. C. Hribar, M. H. Lee, D. Lee and J. A. Burdick, *ACS Nano*, 2011, **5**, 2948–2956.

113 E. B. Dickerson, E. C. Dreaden, X. Huang, I. H. El-Sayed, H. Chu, S. Pushpanketh, J. F. McDonald and M. A. El-Sayed, *Cancer Lett.*, 2008, **269**, 57–66.

114 C. R. Patra, R. Bhattacharya and P. Mukheriee, *J. Mater. Chem.*, 2010, **20**, 547–554.

115 B. Asadishad, M. Vossoughi and I. Alemzadeh, *Ind. Eng. Chem. Res.*, 2010, **49**, 1958–1963.

116 L. Dykman and N. Khlebtsov, *Chem. Soc. Rev.*, 2012, **41**, 2256–2282.

117 R. K. Visaria, R. J. Griffin, B. W. Williams, E. S. Ebbini, G. F. Paciotti, C. W. Song and J. C. Bischof, *Mol. Cancer Ther.*, 2006, **23**, 1014–1020.

118 R. K. Visaria, J. C. Bischof, M. Loren, B. Williams, E. Ebbini, G. Paciotti and R. Griffin, *Int. J. Hyperthermia*, 2007, **23**, 501–511.

119 H. S. Cho, *Phys. Med. Biol.*, 2005, **50**, N163–N173.

120 J. F. Hainfeld, D. N. Slatkin, T. M. Focella and H. M. Smilowitz, *Br. J. Radiol.*, 2006, **79**, 248–253.

121 T. Kong, J. Zeng, X. Wang, X. Yang, J. Yang, S. McQuarrie, A. McEwan, W. Roa, J. Chen and Z. Xing, *Small*, 2008, **4**, 1537–1543.

122 Q. Yang, S. H. Wang, P. W. Fan, L. F. Wang, Y. Di, K. F. Lin and F. S. Xiao, *Chem. Mat.*, 2005, **17**, 5999–6003.

123 M. A. Polizzi, N. A. Stasko and M. H. Schoenfisch, *Langmuir*, 2007, **23**, 4938–4943.

124 J. Kim, S. Seo, K. Kim, M. Kim, T. Ching, K. K. R. and T. Yang, *Nanothechnology*, 2010, **21**, 425102–.

125 J. C. Polf, L. F. Bronk, H. P. Driessen, W. Arap, R. Pasqualini and M. Gillin, *Appl. Phys. Lett.*, 2011, **98**, 193702–193703.

126 W. Roa, X. J. Zhang, L. H. Guo, A. Shaws, X. Y. Hu, Y. P. Xiong, S. Gulavita, S. Patel, X. J. Sun, J. Chen, R. Moore and J. Z. Xing, *Nanotechnology*, 2009, **20**, 375101–.

127 B. Kang, M. A. Mackey and M. A. El-Sayed, *J. Am. Chem. Soc.*, 2010, **132**, 1517–1519.

128 R. van Horssen, T. L. M. Ten Hagen and A. M. M. Eggemont, *Oncologist*, 2006, **11**, 397–408.

129 J. M. Farma, M. Puhlmann, P. A. Soriano, D. Cox, G. F. Paciotti, L. Tamarkin and H. R. Alexander, *Int. J. Cancer*, 2007, **120**, 2474–2480.

130 T. Niidome, N. Yamagata, Y. Okamoto, Y. Akiyama, H. Takahashi, T. Kawano, Y. Katayama and Y. Niidome, *J. Control. Release*, 2006, **114**, 343–347.

131 M. J. Ernsting, M. Murakami, A. Roy and S. D. Li, *J. Controlled Release*, 2013, **172**, 782–794.

132 Y. Pan, S. Neuss, A. Leifert, M. Fischer, F. Wen, U. Simon, G. Schmid, W. Brandau and W. Jahnen-Dechent, *Small*, 2007, **3**, 1941–1949.

133 J. F. Hillyer and R. M. Albrecht, *J. Pharm. Sci.*, 2001, **90**, 1927–1936.

134 W. H. De Jong, W. I. Hagens, P. Krystek, M. C. Burger, A. I. Sips and R. E. Geertsma, *Biomaterials*, 2008, **29**, 1912–1919.

135 B. D. Chithrani, A. A. Ghazani and W. C. W. Chan, *Nano Lett.*, 2006, **6**, 662–668.

136 S. Ganta, H. Devalapally, A. Shahiwala and M. Amiji, *J. Control. Release*, 2008, **126**, 187–204.

137 O. J. Cayre, N. Chagneux and S. Biggs, *Soft Matter*, 2011, **7**, 2211–2234.

138 J. J. Green, E. Chiu, E. S. Leshchiner, J. Shi, R. Langer and D. G. Anderson, *Nano Lett.*, 2007, **7**, 874–879.

139 V. Biju, D. Muraleedharan, K. Nakayama, Y. Shinohara, T. Itoh, Y. Baba and M. Ishikawa, *Langmuir*, 2007, **23**, 10254–10261.

140 H. Mok, J. W. Park and T. G. Park, *Bioconjugate Chem.*, 2008, **19**, 797–801.

141 L. L. Sun, D. J. Liu and Z. X. Wang, *Langmuir*, 2008, **24**, 10293–...

142 E. C. Cho, C. Glaus, J. Chen, M. J. Welch and Y. Xia, *Trends Mol. Med.*, 2010, **16**, 561–573.

143 Z. J. Zhu, H. Wang, B. Yan, H. Zheng, Y. Jiang, O. R. Miranda, V. M. Rotello, B. Xing and R. W. Vachet, *Environ Sci Technol.*, 2012, **20**, 12391–12398.

144 Z. J. Zhu, T. Posati, D. F. Moyano, R. Tang, B. Yan, R. W. Vachet and V. M. Rotello, *Small*, 2012, **10**, 2659–2663.

145 A. M. Jackson, J. W. Myerson and F. Stellacci, *Nature Mat.*, 2004, **3**, 330–336.

146 Z. Wang, R. Lvy, D. G. Fernig and M. Brust, *Bioconjug. Chem.*, 2005, **16**, 497–500.

147 A. G. Tkachenko, H. Xie, D. Coleman, W. Glom, J. Ryan, M. F. Anderson, S. Franzen and D. L. Feldheim, *J. Am. Chem: Soc.*, 2003, **125**, 4700–4701.

148 K. Cho, X. Wang, S. Nie, Z. Chen and D. M. Shin, *Clinic. Cancer Res.*, 2008, **14**, 1310–1316.

149 D. Irvine, *Nature Material*, 2011, **10**, 342–343.

150 P. Ghosh, G. Han, M. De, C. K. Kim and V. M. Rotello, *Adv. Drug Delivery Rev.*, 2008, **60**, 1307–1315.

151 I. Brigger, C. Dubernet and P. Couvreur, *Adv. Drug Deliv. Rev.*, 2002, **54**, 631–651.

152 L. Brannon-Peppas and J. O. Blanchette, *Adv. Drug Deliv. Rev.*, 2004, **56**, 1649–1659.

153 C. Villiers, H. Freitas, R. Couderc, M. B. Villiers and P. Marche, *J. Nanopart, Res.*, 2010, **12**, 55–60.

154 L. Wang, Y. F. Li, L. Zhou, Y. Liu, L. Meng, X. Wu, L. Zhang, B. Li and C. Chen, *Anal. Bioanal. Chem.*, 2010, **396**, 1105–1114.

155 B. J. Marquis, S. A. Love, K. L. Brown and C. L. Haynes, *Analyst*, 2009, **134**, 425–439.

156 A. Nel, T. Xia, L. Madler and N. Li, *Science*, 2006, **311**, 622–627.

157 E. E. Connor, J. Mwamuka, A. Gole, C. J. Murphy and M. D. Wyatt, *Small*, 2005, **1**, 325–327.

158 A. Pan, Y. Leifert, D. Ruau, S. Neuss, J. Bornemann, G. Schmid, W. Brandau, U. Simon and W. Jahnen-Dechent, *Small*, 2009, **5**, 2067–

2076.
159 V. Pokharkar, S. Dhar, D. Bhumkar, V. Mali, S. Bodhankar and B. L. V. Prasad, *J. Biomed. Nanotechnol.*, 2009, **5**, 233–239.
160 N. M. Schaeublin, L. K. Braydich-Stolle, A. M. Schrand, J. M. Miller, J. Hutchison, J. J. Schlager and S. M. Hussain, *Nanoscale*, 2011, **3**, 410–420.
161 R. R. Arvizo, S. Bhattacharyya, R. A. Kudgus, K. Giri, R. Bhattacharya and P. Mukherjee, *Chem. Soc. Rev.*, 2012, **41**, 2943–2970.
162 Y. F. Li and C. Chen, *Small*, 2011, **7**, 2965–2980.
163 A. M. Alkilany and C. J. Murphy, *J. Nanopart. Res.*, 2010, **12**, 2313–2333.